

# Lawrence Berkeley National Laboratory

## Recent Work

### Title

INFRARED LASER ENHANCEMENT OF CHEMICAL REACTIONS VIA COLLISION INDUCED ABSORPTION

### Permalink

<https://escholarship.org/uc/item/9q22w5d9>

### Author

Orel, A.E.

### Publication Date

1979-02-07

INFRARED LASER ENHANCEMENT OF CHEMICAL REACTIONS VIA  
COLLISION INDUCED ABSORPTION

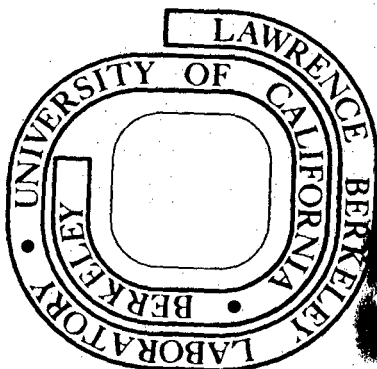
A. E. Orei and W. H. Miller

Prepared for the U. S. Department of Energy  
under Contract W-7405-ENG-48

RECEIVED  
REFERENCE  
BY LABORATORY  
FEB 7 1979  
LIBRARY AND  
DOCUMENTS SECTION

TWO-WEEK LOAN COPY

This is a Library Circulating Copy  
which may be borrowed for two weeks.  
For a personal retention copy, call  
Tech. Info. Division, Ext. 6782



*ed*  
LBL-8575

## **DISCLAIMER**

This document was prepared as an account of work sponsored by the United States Government. While this document is believed to contain correct information, neither the United States Government nor any agency thereof, nor the Regents of the University of California, nor any of their employees, makes any warranty, express or implied, or assumes any legal responsibility for the accuracy, completeness, or usefulness of any information, apparatus, product, or process disclosed, or represents that its use would not infringe privately owned rights. Reference herein to any specific commercial product, process, or service by its trade name, trademark, manufacturer, or otherwise, does not necessarily constitute or imply its endorsement, recommendation, or favoring by the United States Government or any agency thereof, or the Regents of the University of California. The views and opinions of authors expressed herein do not necessarily state or reflect those of the United States Government or any agency thereof or the Regents of the University of California.

Infrared Laser Enhancement of Chemical Reactions via  
Collision Induced Absorption\*

By

A. E. Orel and W. H. Miller<sup>†</sup>

Department of Chemistry, and Materials and Molecular Research Division  
of the Lawrence Berkeley Laboratory, University of California  
Berkeley, CA 94720

### Abstract

We have pointed out previously that an infrared laser will in general enhance the rate of a chemical reaction via a collision induced absorption, even if the reactants themselves are infrared inactive. This paper examines this phenomenon more fully by presenting a simple analytically solvable model which illustrates it and also by presenting the results of classical trajectory calculations we have carried out for the reactions  $X + H_2 \rightleftharpoons HX + H$ , for  $X = H, F, Cl$ . One new feature which is revealed by these calculations is that the polarization of the laser is an important parameter, i.e., certain polarizations are much more effective in enhancing the rate of the reaction than others.

## I. Introduction

It is well-known that the rate of chemical reactions can be enhanced by infrared lasers that vibrationally excite one of the reactants.<sup>1</sup> This requires, of course, that the frequency of the laser coincide with an infrared absorption of one of the reactant molecules.

We have recently pointed out,<sup>2</sup> however, that in general there is a collision induced absorption that enhances the rates of reactions by effectively lowering the activation energy, even if the reactants are infrared inactive. The purpose of this paper is to discuss this phenomenon more fully and to present the results of additional calculations illustrating it.

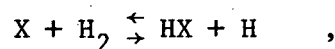
It is easy to understand the phenomenon qualitatively by considering the simple prototype reaction  $\text{H} + \text{H}_2 \rightarrow \text{H}_2 + \text{H}$ . Although the reactants are infrared inactive, it is easy to see that in the transition state region of the potential energy surface the asymmetric stretch motion,  $\vec{\text{H}} \cdots \vec{\text{H}} \cdots \vec{\text{H}}$ , will absorb in the infrared because the system has a non-zero dipole moment that changes with this motion. On the other hand, the symmetric stretch,  $\vec{\text{H}} \cdots \text{H} \cdots \vec{\text{H}}$ , does not absorb infrared radiation since the system develops no dipole moment with this motion. The asymmetric stretch displacement, however, is motion along the reaction coordinate, so the system will absorb energy from the radiation field preferentially in that degree of freedom most effective in promoting the reaction, i.e., in helping it surmount the activation barrier.

It is easy to see that this is a general phenomena since displacement of a transition state along the reaction coordinate is in general the least

symmetric displacement<sup>3</sup> and will thus always be infrared active. It is also clear, however, that the phenomenon requires very intense radiation fields (and thus lasers) since the system is in the transition state region of the potential energy surface for only a short period of time; i.e., the "concentration of transition states" is small.

In addition to interest in this process for the obvious reason of being able to accelerate chemical reactions, it is also interesting because it allows one in effect to "see" (i.e., to interact with) the reactive system in the transition state region itself. In normal scattering experiments one can observe the system only before and after complete collisions. This collision induced absorption is thus the closest in principle that one can come to infrared spectroscopy of a transition state.

Section II first presents a simplified one-dimensional model of the phenomenon that is analytically solvable. This gives a qualitative indication of the nature and order of the magnitude of the effect, i.e., how much the activation energy of a reaction is expected to be lowered by the radiation field. The results of classical trajectory calculations, including the laser field, for the reactions



for  $X = H, F, Cl$  are presented in Section III. The qualitative behavior predicted by the 1-dimensional model of Section II is seen to be borne out by these results.

In closing this Introduction it should be noted that collision induced absorption is a well-known and much studied phenomenon in

itself, e.g., in mixed rare gases.<sup>4</sup> In the present paper our interest is not so much in the absorption spectrum but rather in how the absorption affects the collision dynamics, e.g., by changing non-reactive trajectories into reactive ones. Also, there has been considerable interest in the effect on collision processes caused by laser-induced electronic excitation;<sup>5</sup> this usually (but not necessarily) involves a visible laser and, of course, requires the existence of an appropriate electronically excited potential energy surface.



## II. One Dimensional Model

To obtain a simple analytic solution to serve as a qualitative guide to more quantitative calculations, we carry out in this section a calculation for the simplest possible version of the process we are describing. We thus assume for the present (1) that the potential energy surface is separable in the region of the transition state, (2) that only motion along the reaction coordinate is optically active, and (3) that the potential barrier in the reaction coordinate is parabolic. A further approximation is (4) that the effect of the radiation field of the motion along the reaction coordinate is treated by lowest order perturbation theory. The calculation is carried out, as are the numerical calculations reported in the next section, within the framework of the classical theory<sup>6</sup> recently developed to treat the interaction of molecular systems with electromagnetic radiation.

Letting  $x$  denote the coordinate for motion along the reactive direction, consider a classical trajectory beginning at  $x_1$  (cf. Figure 1) at  $t = 0$ , with initial momentum  $p_1$  ( $x_1 < 0$  and  $p_1 > 0$ ). The potential energy barrier  $V(x)$  is parabolic,

$$V(x) = -\frac{1}{2} m\omega_b^2 x^2, \quad (2.1)$$

so that the initial energy in this degree of freedom,  $E_1$ , is

$$E_1 = \frac{p_1^2}{2m} - \frac{1}{2} m\omega_b^2 x_1^2. \quad (2.2)$$

If  $E_1 < 0$ , as shown in Figure 1, then the field-free trajectory will clearly be non-reactive.

$N_1$  and  $Q_1$  are the initial quantum number and phase of the radiation field, and we first determine the trajectory  $x(t; x_1, p_1, N_1, Q_1)$ , noting that it depends on the various initial conditions. According to the perturbation result obtained in reference 6,  $x(t)$  is given through first order in the interaction between molecule and radiation field by

$$x(t) = x_0(t) + \Delta x(t) \quad , \quad (2.3)$$

where  $x_0(t)$  is the field-free trajectory, which in this case is

$$x_0(t) = x_1 \cosh(\omega_b t) + \frac{p_1}{m\omega_b} \sinh(\omega_b t) \quad , \quad (2.4)$$

and where  $\Delta x(t)$  is the correction caused by the radiation field:

$$\begin{aligned} \Delta x(t) = \sqrt{\frac{8\pi\hbar\omega N_1}{V}} \int_0^t dt' \left[ \frac{\partial x_0(t; x_1, p_1)}{\partial p_1} \frac{\partial x_0(t'; x_1, p_1)}{\partial x_1} \right. \\ \left. - \frac{\partial x_0(t; x_1, p_1)}{\partial x_1} \frac{\partial x_0(t'; x_1, p_1)}{\partial p_1} \right] \mu'(x_0(t')) \sin(\omega t' + Q_1); \end{aligned} \quad (2.5)$$

$\mu(x)$  is the dipole moment of the molecular system as a function of  $x$ .

Utilizing Eq. (2.4), Eq. (2.5) becomes

$$\Delta x(t) = \sqrt{\frac{8\pi\hbar\omega N_1}{V}} (m\omega_b)^{-1} \int_0^t dt' \mu'(x_0(t')) \sinh[\omega_b(t-t')] \sin(\omega t' + Q_1) \quad . \quad (2.6)$$

To determine whether the trajectory is reactive or not, we consider the limit  $t \rightarrow +\infty$  to see if  $x(t \rightarrow \infty) \rightarrow +\infty$  (reactive) or  $-\infty$  (non-reactive). Eqs. (2.4) and (2.6) show that as  $t \rightarrow +\infty$ ,

$$x(t) \equiv x_0(t) + \Delta x(t)$$

$$\sim \frac{1}{2} e^{\omega_b t} \left[ x_1 + \frac{p_1}{m\omega_b} + \sqrt{\frac{8\pi\hbar\omega N_1}{v}} (m\omega_b)^{-1} \int_0^\infty dt' \mu'(x_0(t')) e^{-\omega_b t'} \sin(\omega t' + Q_1) \right]. \quad (2.7)$$

To simplify matters further we also assume that the dipole derivative is constant,  $\mu'(x) = \mu'$ , so that

$$\int_0^\infty dt' \mu'(x_0(t')) e^{-\omega_b t'} \sin(\omega t' + Q_1) = \frac{\mu' [\omega \cos Q_1 + \omega_b \sin Q_1]}{\omega^2 + \omega_b^2}, \quad (2.8a)$$

and take  $x_1$  large enough so that

$$x_1 + \frac{p_1}{m\omega_b} = x_1 + (2mE_1 + m^2\omega_b^2 x_1^2)^{1/2} / (m\omega_b) \approx E_1 / (m\omega_b^2 |x_1|) \quad (2.8b)$$

Eq. (2.7), with Eq. (2.8), then implies that the trajectory is reactive or not depending on whether the following quantity is positive or negative:

$$\frac{E_1}{m\omega_b^2 |x_1|} + \sqrt{\frac{8\pi\hbar\omega N_1}{V}} \frac{\mu'}{m\omega_b} \frac{(\omega\cos Q_1 + \omega_b\sin Q_1)}{\omega^2 + \omega_b^2} \quad (2.9)$$

The characteristic function for reaction  $\chi_R(N_1, Q_1; E_1)$ , which is 1 for reactive trajectories and 0 for non-reactive ones, is thus given by

$$\chi_R(N_1, Q_1; E_1) = h \left[ E_1 + \frac{\hbar\omega_R\omega_b}{\omega^2 + \omega_b^2} (\omega\cos Q_1 + \omega_b\sin Q_1) \right] \quad (2.10)$$

where  $h(\ )$  is the usual step-function,

$$h(z) = \begin{cases} 1, & z > 0 \\ 0, & z < 0 \end{cases} \quad ,$$

and where  $\omega_R$  is the Rabi frequency for the transition,

$$\hbar\omega_R \equiv \sqrt{\frac{8\pi\hbar\omega N_1}{V}} |\mu' x_1| \quad (2.11)$$

The net reaction probability is obtained by averaging  $\chi_R$  over the initial phase of the field,

$$P_R(N_1, E_1) = (2\pi)^{-1} \int_0^{2\pi} dQ_1 \chi_R(N_1, Q_1; E_1) \quad (2.12)$$

and it is easy to show that with  $\chi_R$  given by Eq. (2.10) the result is

$$P_R(N_1, E_1) = \frac{1}{2} + \sin^{-1}(E_1/E_{th})/\pi \quad (2.13)$$

where  $E_{th}$ , the threshold for reaction, is given by

$$E_{th} = -\hbar\omega_R(1 + \omega^2/\omega_b^2)^{-1/2} \quad (2.14)$$

Equations (2.13) and (2.14) are the principle results of this model calculation, and they should be regarded as qualitative, order-of-magnitude indicators. Figure 2 shows the reaction probability of Eq. (2.13) as a function of energy  $E_1$ , compared to the field-free result. The important feature is that the threshold for the reaction has been depressed by the presence of the radiation field. Eq. (2.14) shows that the amount by which the threshold energy is lowered is roughly  $\hbar\omega_R$ .

The numerical classical trajectory calculations described in the next section also show the qualitative behavior described by Eqs. (2.13) and (2.14).

The dependence of this absorption on the frequency of the laser is also easy to understand qualitatively within the framework of this one-dimensional picture. For a reactive trajectory, i.e., one that passes over the barrier in Figure 1, the time dependence of the molecular dipole moment will be of the form sketched in Figure 3a. (This would be the case, for example, for the  $H + H_2 \rightarrow H_2 + H$  reaction.) In the one photon perturbative limit the absorption coefficient, i.e., the probability of the system absorbing a photon, is proportional to the square modulus of the Fourier transform of  $\mu(t)$ :

$$I(\omega) \propto \left| \int_{-\infty}^{\infty} dt e^{i\omega t} \mu(t) \right|^2 \quad (2.15)$$

Suppose, for example,

$$\mu(x) = \mu' x \exp(-\frac{1}{2} x^2/a^2) \quad (2.16a)$$

and

$$x(t) = vt \quad (2.16b)$$

Eq. (2.15) then gives

$$I(\omega) \propto \omega^2 \exp(-\omega^2 a^2/v^2) \quad (2.17)$$

which is sketched in Figure 3b. The probability of absorption is largest in this case for

$$\omega = v/a \quad ; \quad (2.18)$$

frequencies above or below this value are not as effective in promoting the reactive, and this optimum laser frequency is seen to vary monotonically with the collision energy.

III. Classical Trajectory Calculations for  $X + H_2 \rightleftharpoons HX + H$  ( $X = H, F, Cl$ )

To obtain a more quantitatively reliable characterization of how this collision induced absorption enhances the rate of reactions, we have carried out classical trajectory calculations within the framework of the theoretical model developed in reference 6. In this model the molecular degrees of freedom, and also the radiation field--approximated as a single mode laser--are treated by classical mechanics, i.e., by numerically integrating Hamilton's equations for the complete system, molecules plus radiation field.

For the case of a collinear A + BC collision in a single mode radiation field, the classical Hamiltonian for the complete system is

$$H(p_R, R, p_r, r, p_X, X) = \frac{p_R^2}{2\mu} + \frac{p_r^2}{2m} + \frac{p_X^2}{2} + V(r, R) + \frac{1}{2} \omega^2 X^2 - \sqrt{\frac{4\pi\omega^2}{V}} \mu(r, R) X \quad , \quad (3.1)$$

where  $(R, p_R)$ ,  $(r, p_r)$ , and  $(X, p_X)$  are the coordinates and momenta for the translation of A relative to the center of mass of BC, the relative vibration of B-C, and the radiation field, respectively.  $\mu$  and  $m$  are the corresponding reduced masses,  $\omega$  is the frequency of the laser,  $V$  the volume of the radiation cavity,  $\mu(r, R)$  is the dipole moment of the A-B-C system as a function of its configuration, and  $V(r, R)$  is the field-free potential energy surface for the A-B-C system. (For the three-dimensional case  $\mu(r, R)$  is replaced by  $\vec{\mu}(\vec{r}, \vec{R}) \cdot \hat{\epsilon}$ , where  $\vec{\mu}$  is the dipole moment vector of the molecular system and  $\hat{\epsilon}$  is the polarization vector of

the radiation field.) One sees that the radiation field enters in this model as simply one additional mechanical degree of freedom, a harmonic oscillator, that is coupled to the molecular degrees of freedom. It is convenient to replace the field variables  $(X, p_X)$  by the action-angle variables  $(N, Q)$ , defined in the usual manner,

$$X = \sqrt{\frac{2\hbar(N + \frac{1}{2})}{\omega}} \sin Q \quad (3.2a)$$

$$P = \sqrt{2\hbar\omega(N + \frac{1}{2})} \cos Q \quad , \quad (3.2b)$$

and the Hamiltonian then becomes

$$H(p_R, R, p_r, r, N, Q) = \frac{p_R^2}{2\mu} + \frac{p_r^2}{2m} + V(r, R) + \hbar\omega(N + \frac{1}{2}) - \sqrt{\frac{8\pi\hbar\omega N}{V}} \mu(r, R) \sin Q \quad . \quad (3.3)$$

$N$  is the quantum number of the radiation field oscillator, i.e., the number of photons in the field, and  $Q$  is the phase of the field.

The initial conditions for the classical trajectories are

$$\begin{aligned} R(t_1) &= \text{large } (>> 0) \\ p_R(t_1) &= -\sqrt{2\mu E_1} \\ N(t_1) &= N_1 \\ Q(t_1) &= Q_1 \\ r(t_1) &= r(n_1, q_1) \\ p_r(t_1) &= p(n_1, q_1) \quad , \end{aligned} \quad (3.4)$$

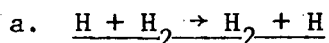


where  $r(n,q)$  and  $p(n,q)$  are the algebraic functions expressing the vibrational variables  $(r,p_r)$  in terms of the vibrational action-angle variables  $(n,q)$ . (For the present examples the vibrational potential of the isolated BC molecule is a Morse potential so that the functions  $r(n,q)$  and  $p(n,q)$  are those given before.<sup>7</sup>)  $E_1$  is the initial translational energy, and the quantum numbers  $n_1$  and  $N_1$  are integers, the initial vibrational state of BC and the initial number of photons in the radiation field, respectively.

To carry out the usual quasi-classical type calculation<sup>8</sup> it is useful to define the characteristic function for reaction  $\chi_R(q_1, Q_1, n_1, N_1; E_1)$ , which is 1 if the trajectory with these initial conditions is reactive, and 0 if it is non-reactive. The total reaction probability from the initial vibrational state  $n_1$ , with initial translational energy  $E_1$ , and with  $N_1$  photons initially in the radiation field, is then given in the quasiclassical framework by

$$P_R(n_1, N_1; E_1) = (2\pi)^{-2} \int_0^{2\pi} dq_1 \int_0^{2\pi} dQ_1 \chi_R(q_1, Q_1, n_1, N_1; E_1) \quad (3.5)$$

The above discussion is modified in a reasonably obvious fashion to treat the three-dimensional version of an A + BC collision process.



Although this reaction is not of great interest in itself, it is the simplest prototype chemical reaction, and since it is so well-characterized and since the reactants are infrared inactive, it is a good example to illustrate this collisionally induced absorption. Preliminary calculations

on this system have been published elsewhere.<sup>2</sup>

The Porter-Karplus<sup>9</sup> potential energy surface was employed in the trajectory calculations reported here, and the following dipole moment function was used:

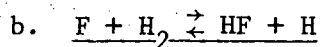
$$\mu(r,R) = s \operatorname{sech}^2(s) \quad , \quad (3.6)$$

where

$$s = \frac{3}{2} r - R \quad ;$$

$s$  is the asymmetric stretch coordinate at the saddle point of the potential energy surface. Although not quantitative, this dipole moment function is qualitatively correct, and an overall multiplicative constant is absorbed in the definition of  $\omega_R$ . Three field strengths were studied, corresponding to  $\hbar\omega_R = 0.001, 0.01, \text{ and } 0.1 \text{ eV}$ . At the lowest value little effect is observable, but for  $\hbar\omega_R = .01 \text{ eV}$  the reactive threshold was lowered as expected and as explained by the model in Section II. For the largest laser power ( $\hbar\omega_R = 0.1 \text{ eV}$ ) the effect is most significant, and these results are shown in Figure 4.

The variation of threshold lowering with laser frequency is summarized in Table I. Since the dipole moment is similar to that shown in Figure 3a, it was expected that the absorption would be similar to that of Figure 3b and that the effect would thus peak at some finite laser frequency. This is observed in Table I, the optimum laser frequency being  $\sim 500 \text{ cm}^{-1}$ .



This system has a very asymmetric barrier. In the forward direction

it is enhanced by translational energy, and in the backward direction HF will not react collinearly unless excited to the  $v = 2$  vibrational state.

Polanyi's SE1 surface,<sup>10</sup> a semi-empirical modified LEPS (London-Eyring-Polanyi-Sato) potential surface, was used in this calculation, the parameters for which are summarized in Table II. The dipole moment function for F-H-H was approximated as the sum of the two individual H-F dipole moments, where the H-F dipole moment as a function of internuclear distance is the theoretical result of Lie<sup>11</sup> which was fit to the form

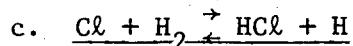
$$\mu(r) = e^{-\alpha r} \sum_{n=0}^5 c_n r^n ; \quad (3.7)$$

the parameters of this fit are given in Table III.

The collinear results for  $F + H_2(v=0) \rightarrow HF + H$  are shown in Figure 5 for  $\hbar\omega_R = 0.1$  eV, corresponding to a laser power of  $\sim 30$  gigawatts/cm<sup>2</sup>; they are seen to be qualitatively similar to  $H + H_2 \rightarrow H_2 + H$  above. Similar results for the reverse reaction,  $H + HF(v) \rightarrow H_2 + F$ , are shown in Figure 6 for  $v = 2$ . There is no reaction, with or without the laser, for  $v = 0, 1$ , and for  $v = 3$  the increased vibrational energy damps out the laser effect.

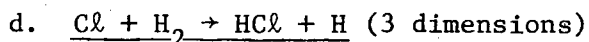
In contrast to the  $H + H_2$  reaction, the variation of the dipole moment with time for  $F + H_2 \xrightarrow{\text{laser}} HF + H$  behaves qualitatively as a smooth step-function, i.e., it rises from zero to a finite value along the reaction coordinate, unlike that in Figure (3a). In this case its Fourier transform is a monotonically decreasing function of frequency  $\omega$ ; i.e.,  $I(\omega)$  increases as  $\omega$  decreases. In this case one thus expects the effect of the collision induced absorption to increase monotonically with decreasing laser frequency.

The dependence of the threshold lowering on laser frequency for this reaction (cf. Table I) does indeed show this behavior.



The parameters for the modified LEPS potential surface used in the calculation are summarized in Table II.<sup>12</sup> The dipole moment function of HCl was fit to the same general shape as the HF dipole moment but scaled so that the correct value was obtained for both the dipole moment and dipole moment derivative at the equilibrium bond distance. The parameters are summarized in Table III.

The results for collinear  $\text{Cl} + \text{H}_2(v=0) \rightarrow \text{HCl} + \text{H}$  are shown in Figure 7 for  $\hbar\omega_R = 0.1$  eV and for 0.01 eV, and the effect of varying the laser frequency is summarized in Table I. Results for the reverse reaction,  $\text{H} + \text{HCl}(v=0) \rightarrow \text{H}_2 + \text{Cl}$ , are shown in Figure 8 for  $\hbar\omega_R = 0.1$  eV. The overall behavior is similar to that of  $\text{F} + \text{H}_2$  discussed above.



Finally, fully three dimensional trajectory calculations were carried out for  $\text{Cl} + \text{H}_2(v=0, j=0) \rightarrow \text{HCl} + \text{H}$  for  $\hbar\omega_R = 0.1$  eV. The interest here is to see if the effect of threshold lowering is diminished by the additional degrees of freedom present for the three dimensional collision system. The potential surface and dipole moment function are the same as those used above for the collinear calculation.

Another interesting feature of the three-dimensional system is the effect of polarization of the laser beam. One thus imagines a molecular beam experiment with beams of Cl and of  $\text{H}_2$  crossed at right angle, and with the laser beam perpendicular to the two of them; i.e., the three

beams form the edges of a cube. The electric field vector of the laser beam, i.e., the polarization vector, then lies in the plane of the two molecular beams, and we consider the two canonical cases that the polarization vector is parallel to the initial relative velocity vector of Cl and H<sub>2</sub> or that it is perpendicular to the initial relative velocity vector. (The effect of laser polarization for the case of electronic excitation during a collision has been discussed by Light and Szöke.<sup>5d</sup>)

If the reaction proceeds primarily through nearly collinear geometries and is limited to small impact parameters, then one expects the parallel polarization to be most effective in enhancing the reaction since the dipole moment function  $\vec{\mu}(\vec{r}, \vec{R})$  would then be approximately parallel to the polarization vector  $\hat{\epsilon}$ , so that  $|\hat{\epsilon} \cdot \vec{\mu}|$  has its largest value. Conversely, perpendicular polarization would cause  $\vec{\mu}$  to be approximately perpendicular to  $\hat{\epsilon}$ , so that  $|\hat{\epsilon} \cdot \vec{\mu}| \sim 0$ .

Figure 9 shows the reactive cross section as a function of initial translation energy for the field-free case and for parallel and perpendicular polarizations. One sees that parallel polarization is indeed more effective--perpendicular polarization gives almost no effect at all--and one sees that the effect is not at all diminished in three dimensions.

The frequency dependence of the threshold lowering is given in Table I and is similar to the above results for the collinear case.

#### IV. Concluding Remarks

The classical trajectory calculations for the various  $A + BC \rightarrow AB + C$  reactions described in Section III give a good characterization of how this collision induced absorption affects the reaction probability, most significantly by lowering the activation energy for reaction. The three-dimensional calculations for  $Cl + H_2 \rightarrow HCl + H$  showed (1) that the effect is not significantly diminished by the additional degrees of freedom present in the three-dimensional case, and (2) that the polarization of the laser field can be a very interesting parameter of the process. The calculations also confirm that very high laser powers are required, e.g.,  $10^{10}$ - $10^{12}$  watts/cm<sup>2</sup>, because the absorption must take place within a collision time.

With regard to future directions, there is one aspect of the phenomenon that we have not yet pursued, and that is the absorption spectrum itself, i.e., the experiment in which one detects the photons rather than the molecules. This is the precise analog of well-known non-reactive collision induced absorption. In this case the absorption is essentially a probe of the collision dynamics, and it is an interesting probe since it takes place in the interaction (or transition state) region of the potential energy surface.

If, for example, the reaction mechanism is direct, as the examples studied in Section III, then the collision induced absorption spectrum will be broad (cf. Figure 3b), but if a long-lived collision complex is formed, then the spectrum will be structured. In either case qualitative information about the reaction dynamics is easily extracted from such measurements--e.g., the width of the absorption lines is related to the lifetime of the collision complex--but it is likely that quantitative analysis of the spectrum would require scattering calculations on model potential energy surfaces.

Acknowledgments

This work has been supported by the Division of Chemical Sciences, Office of Basic Energy Sciences, U.S. Department of Energy, and all calculations were carried out on a Harris Slash Four minicomputer funded by a National Science Foundation Grant CHE-7622621. WHM also acknowledges support of the Miller Institute of Sciences.

References

\* Preliminary results of this work were presented at the D. L. Bunker Memorial Symposium in the 175<sup>th</sup> National Meeting of the American Chemical Society, Anaheim, California, March 12-17, 1978, and also at the 11<sup>th</sup> International Symposium on Rarefied Gas Dynamics, Cannes, France, July 3-8, 1978.

† Camille and Henry Dreyfus Teacher-Scholar.

1. For example, T. J. Odiorne, P. R. Brooks and J. V. V. Kasper, J. Chem. Phys. 55, 1980 (1970).
2. A. E. Orel and W. H. Miller, Chem. Phys. Lett. 57, 362 (1978).
3. P. Pechukas, J. Chem. Phys. 64, 1516 (1976).
4. See, for example, E. Bar-Ziv and S. Weiss, J. Chem. Phys. 64, 2412, 2417 (1976).
5. See, for example, (a) N. M. Kroll and K. M. Watson, Phys. Rev. A 13, 1018 (1976); (b) J. M. Yuan, T. F. George, and F. J. McLafferty, Chem. Phys. Lett. 40, 163 (1976); (c) A. M. F. Lau, Phys. Rev. A 13, 139 (1976); (d) J. Light and A. Szöke, Phys. Rev. A 18, 1363 (1978).
6. W. H. Miller, J. Chem. Phys. 69, 2188 (1978).
7. C. C. Rankin and W. H. Miller, J. Chem. Phys. 55, 3150 (1971).
8. See, for example, R. N. Porter and L. M. Raff, in "Dynamics of Molecular Collisions", Vol. 2 of Modern Theoretical Chemistry, ed., W. H. Miller Plenum, N.Y., 1976, pp. 1-50.
9. R. N. Porter and M. Karplus, J. Chem. Phys. 40, 1105 (1964).
10. J. C. Polanyi and J. L. Schreiber, Chem. Phys. Lett. 29, 319 (1974).
11. G. C. Lie, J. Chem. Phys. 60, 2991 (1974).
12. A. Persky, J. Chem. Phys. 66, 2932 (1977).



Table I. Dependence of Threshold Lowering on Laser Frequency.

Laser Frequency ( $\text{cm}^{-1}$ )	$\Delta E_{\text{th}}$ (eV) <sup>a</sup>					
	<u>H + H<sub>2</sub></u>	<u>F + H<sub>2</sub></u>	<u>H + HF</u>	<u>Cl + H<sub>2</sub></u>	<u>H + HCl</u>	<u>Cl + H<sub>2</sub></u> 3-dimensional
47	--	--	--	0.13	--	--
94	0.05	> 0.05	0.03	0.12	0.04	0.07
219	0.06	--	--	--	--	--
472	--	0.01	0.03	0.05	0.02	.06
519	0.09	--	--	--	--	--
768	0.08	--	--	--	--	--
944	0.07	0	0.02	0.01	0.01	0.01
2195	0.01	--	--	--	--	--

<sup>a</sup>Amount by which the threshold of the reaction is lowered by a laser field of a power corresponding to  $\hbar\omega_R = 0.1$  eV.

Table II. LEPS Parameters for Potential Energy Surfaces.

	H-H-F		H-H-Cl	
	<u>HF</u>	<u>HH</u>	<u>HCl</u>	<u>HH</u>
$D_e$ (kcal/mole)	140.5	109.5	106.41	109.43
$\beta$ ( $\text{\AA}^{-1}$ )	2.22	1.94	1.87	1.94
$r_0$ ( $\text{\AA}$ )	0.917	0.742	1.27	0.742
$\Delta$	0.150	0.080	0.187	0.167

Table III. Parameters for the HX Dipole Moment Function<sup>a</sup> in Eq. (3.7).

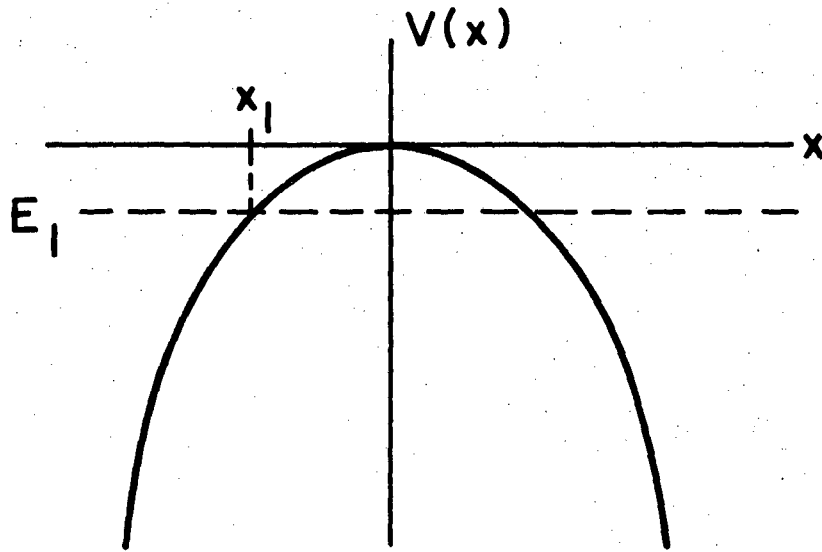
<u>n</u>	<u>C<sub>n</sub></u>	
	<u>HF</u>	<u>HCl</u>
0	2.35	- 236.95
1	- 3.40	1151.69
2	- 40.16	- 2011.50
3	112.15	1631.43
4	- 87.97	- 635.97
5	30.31	101.24

$$\alpha = 2.5 \text{ bohr}^{-1}.$$

<sup>a</sup>Unit of  $\mu(r)$  are  $e a_0$ .

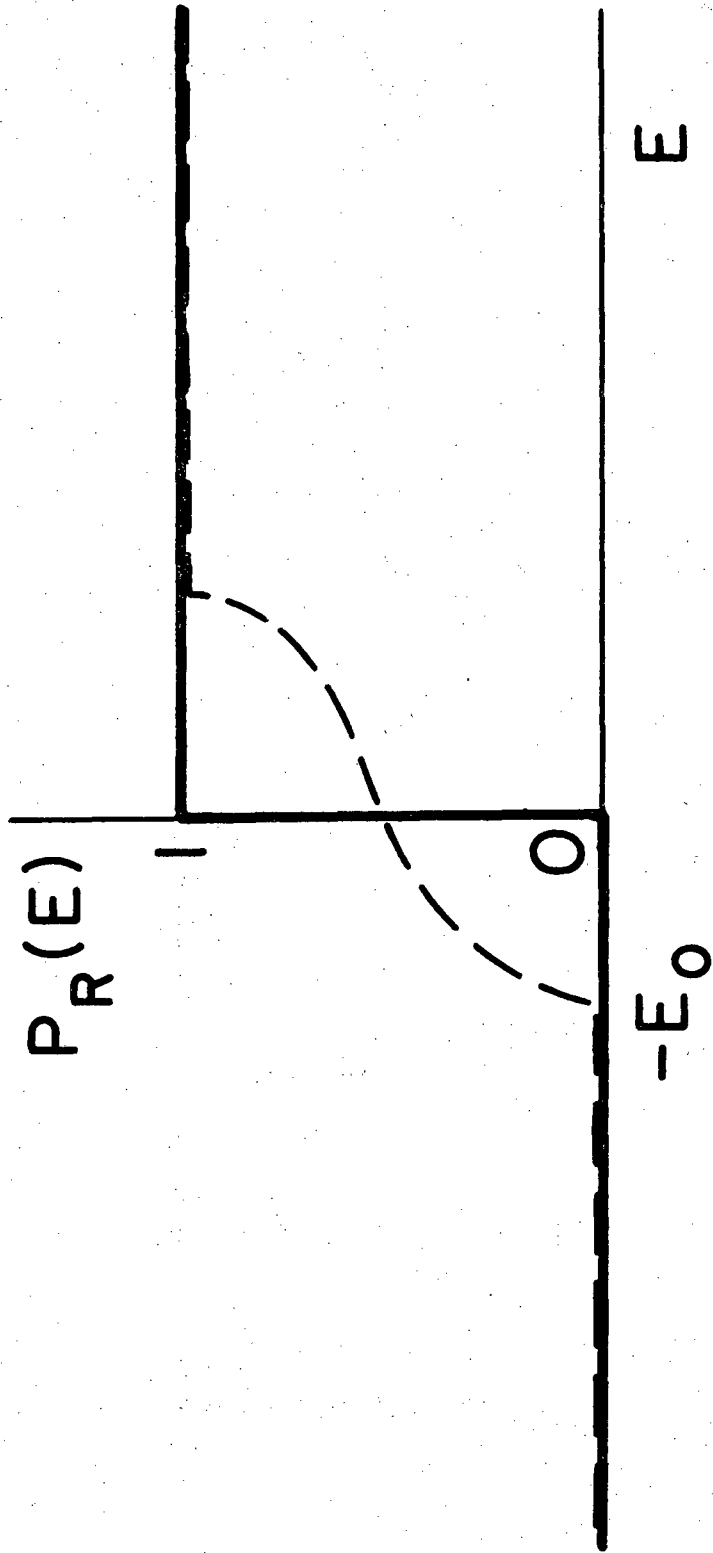
Figure Captions

1. Sketch of a one-dimensional potential energy barrier.  $x_1$  is the initial position and  $E_1$  the initial energy.
2. Reaction probability as a function of initial translational energy [as given by Eq. (2.13)] for the one-dimensional model problem.
3. (a) Sketch of the time dependence of the dipole moment of the H-H-H system along a reactive trajectory  $H + H_2 \rightarrow H_2 + H$ .  
(b) Sketch of the absorption spectrum corresponding to the time-dependent dipole in (a).
4. Reaction probability for the collinear  $H + H_2 \rightarrow H_2 + H$  reaction as a function of initial translational energy, without the laser field (—) and with it (---);  $\hbar\omega = 944 \text{ cm}^{-1}$  and  $\hbar\omega_R = 0.1 \text{ eV}$ .
5. Same as Figure 4 except for the reaction  $F + H_2(v=0) \rightarrow HF + H$ ;  $\hbar\omega = 94 \text{ cm}^{-1}$  and  $\hbar\omega_R = 0.1 \text{ eV}$ .
6. Same as Figure 4 except for the reaction  $H + HF(v=2) \rightarrow H_2 + F$ ;  $\hbar\omega = 94 \text{ cm}^{-1}$  and  $\hbar\omega_R = 0.1 \text{ eV}$ .
7. Same as Figure 4 except for the reaction  $Cl + H_2(v=0) \rightarrow HCl + H$ ;  $\hbar\omega = 94 \text{ cm}^{-1}$ , and  $\hbar\omega_R = 0.01 \text{ eV}$  and  $0.1 \text{ eV}$  as labeled.
8. Same as Figure 4 except for the reaction  $H + HCl(v=0) \rightarrow H_2 + Cl$ ;  $\hbar\omega = 94 \text{ cm}^{-1}$  ( $\cdots$ ),  $472 \text{ cm}^{-1}$  (---), and  $\hbar\omega_R = 0.1 \text{ eV}$ .
9. Reactive cross section for the three-dimensional reaction  $Cl + H_2 \rightarrow HCl + H$  as a function of initial translational energy, without the laser (—) and with it (---);  $\parallel$  and  $\perp$  indicate the cases of parallel and perpendicular polarization vector of the laser to the initial relative velocity vector, respectively.  $\hbar\omega = 94 \text{ cm}^{-1}$ ,  $\hbar\omega_R = 0.1 \text{ eV}$ .



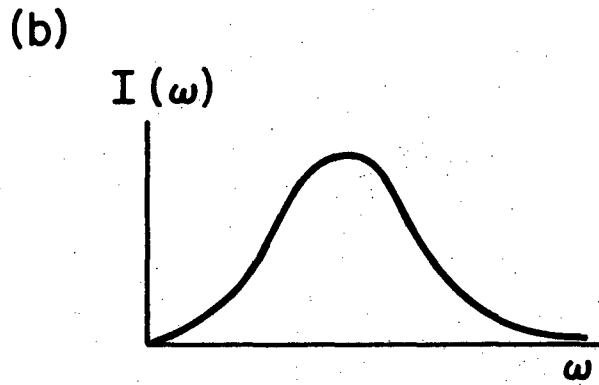
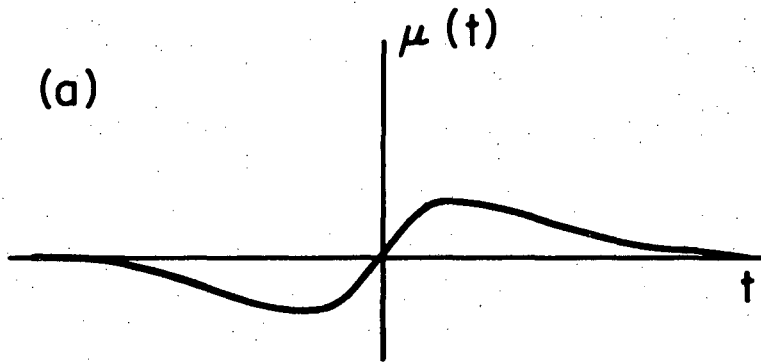
XBL 7812-14071

Figure 1



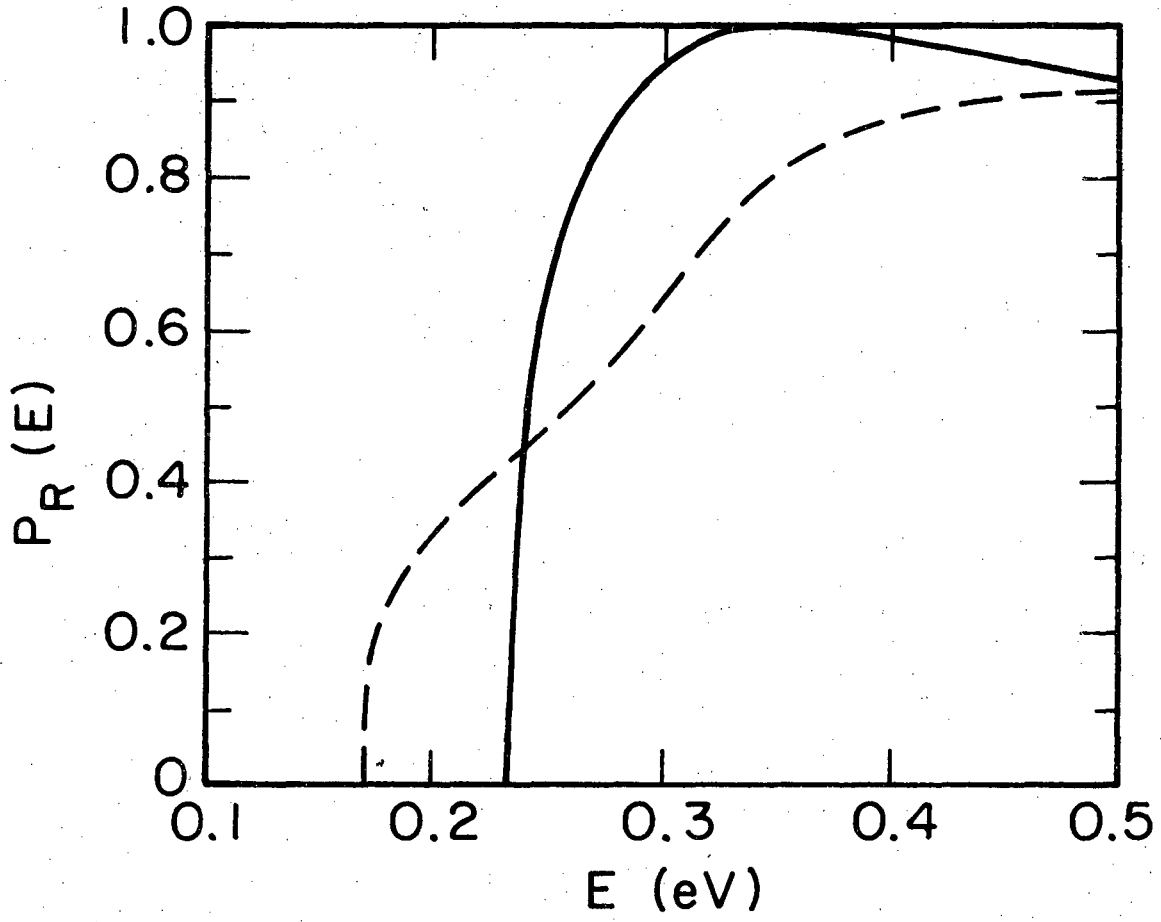
XBL 783-7788

Figure 2



XBL 7812-14072

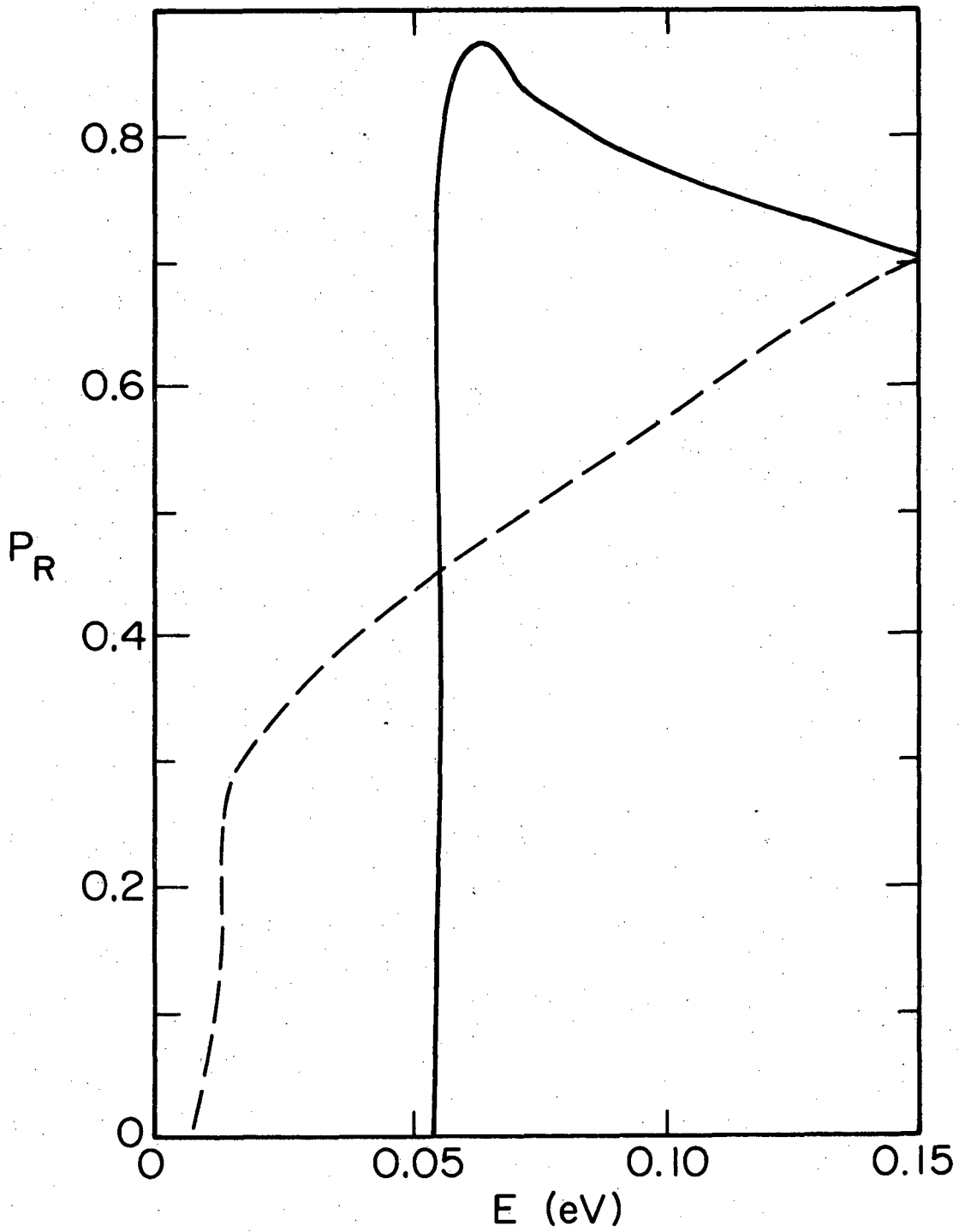
Figure 3



XBL 783-7789

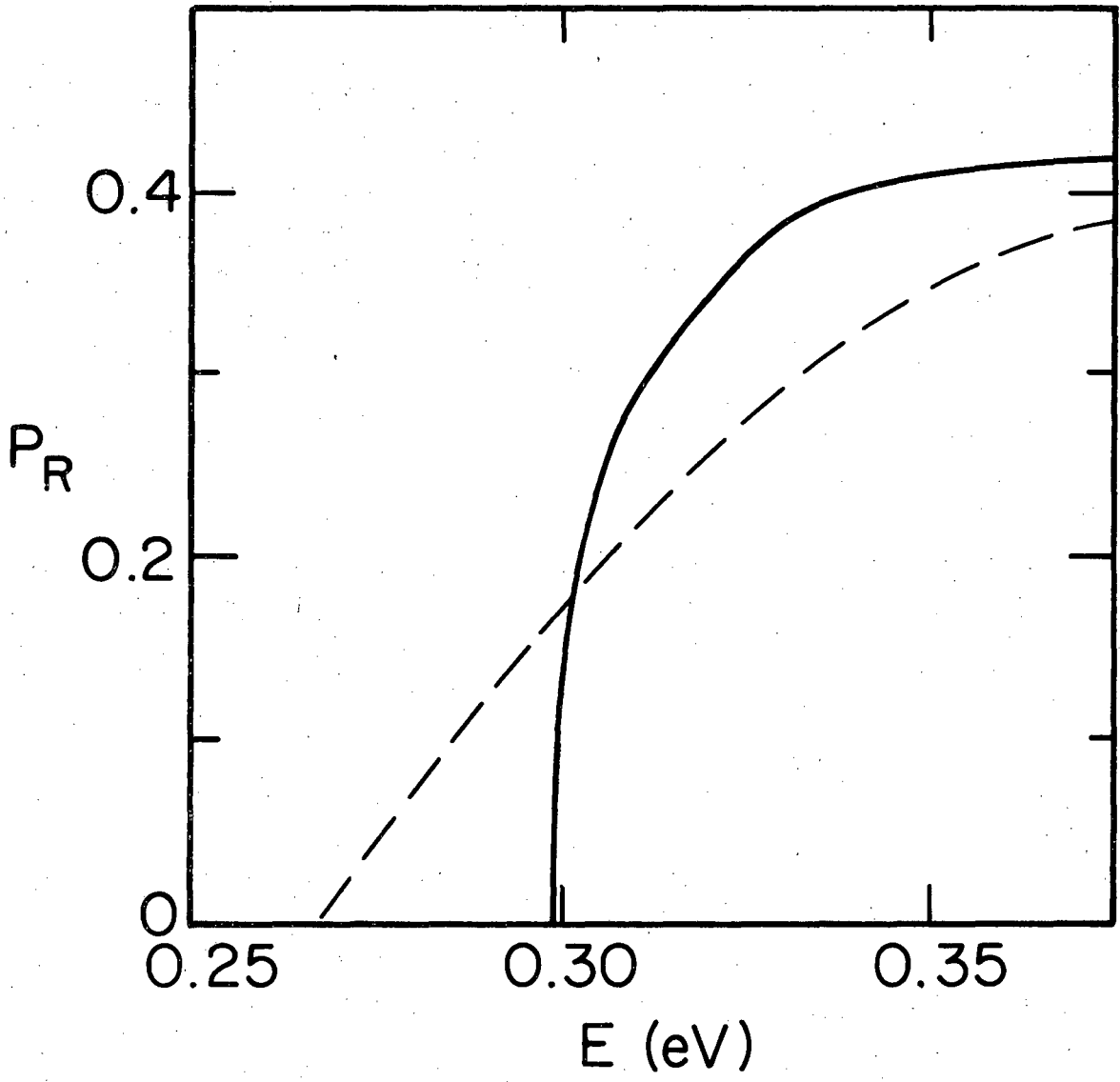
Figure 4





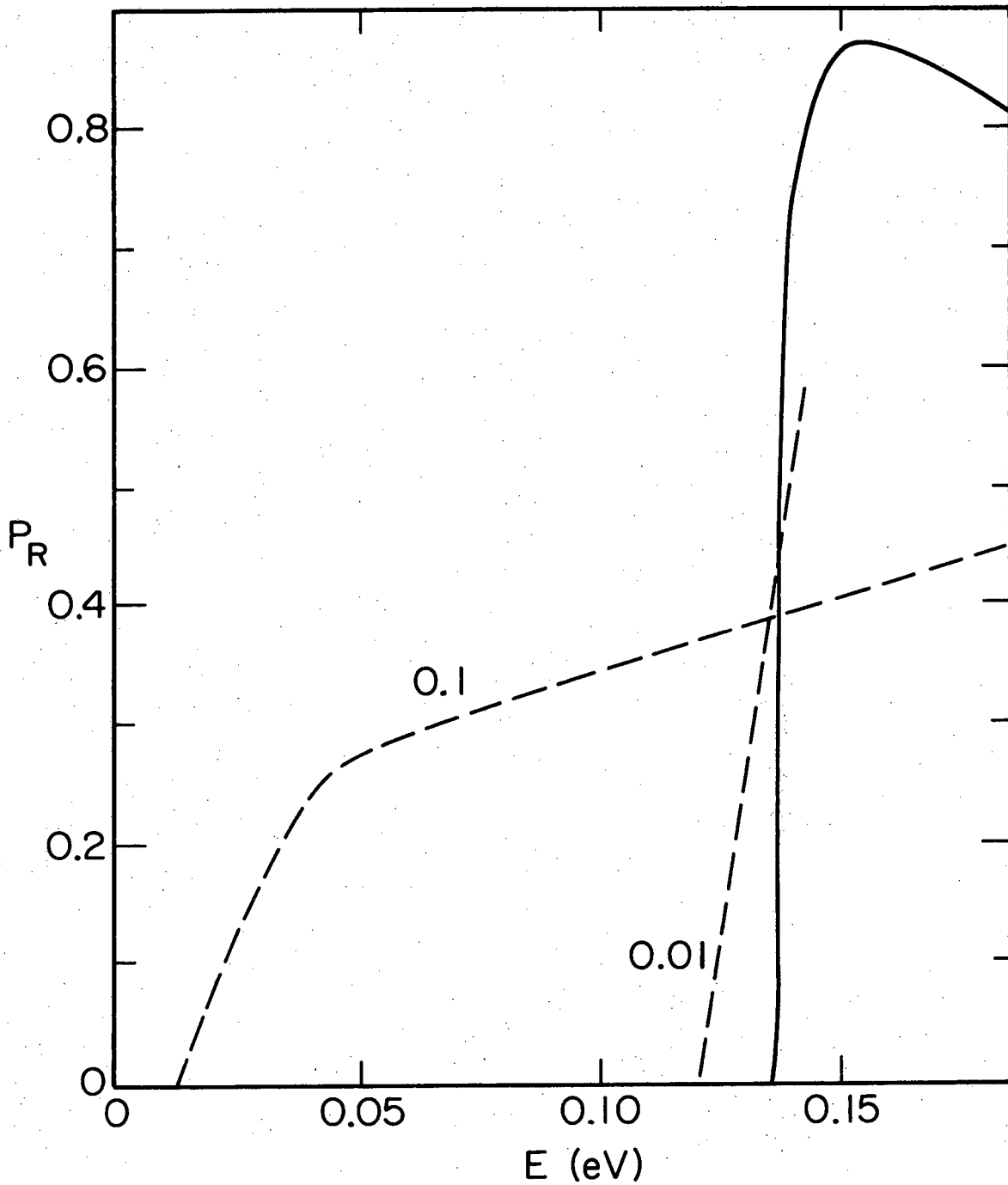
XBL 7810-12115

Figure 5



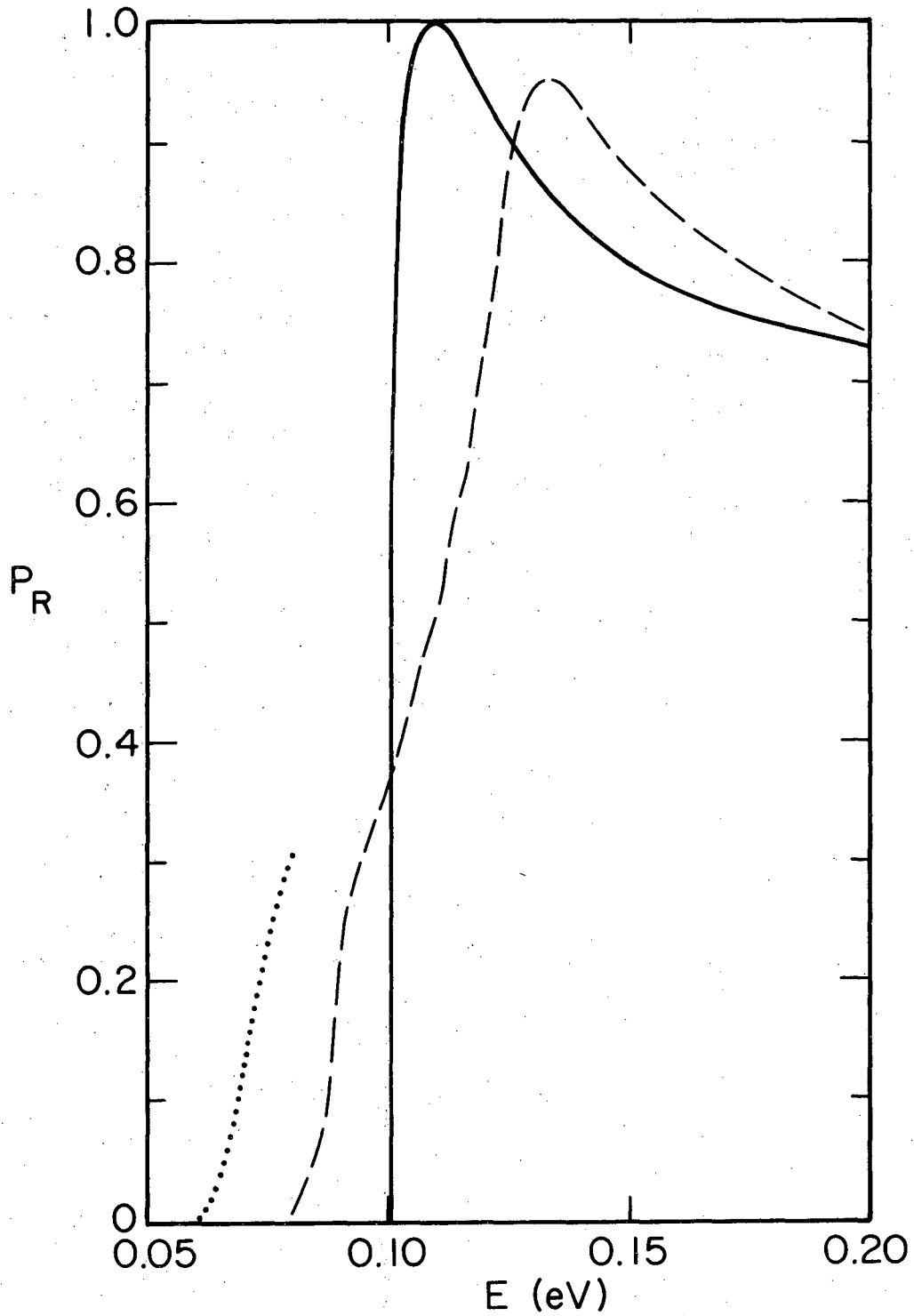
XBL 7812-14073

Figure 6



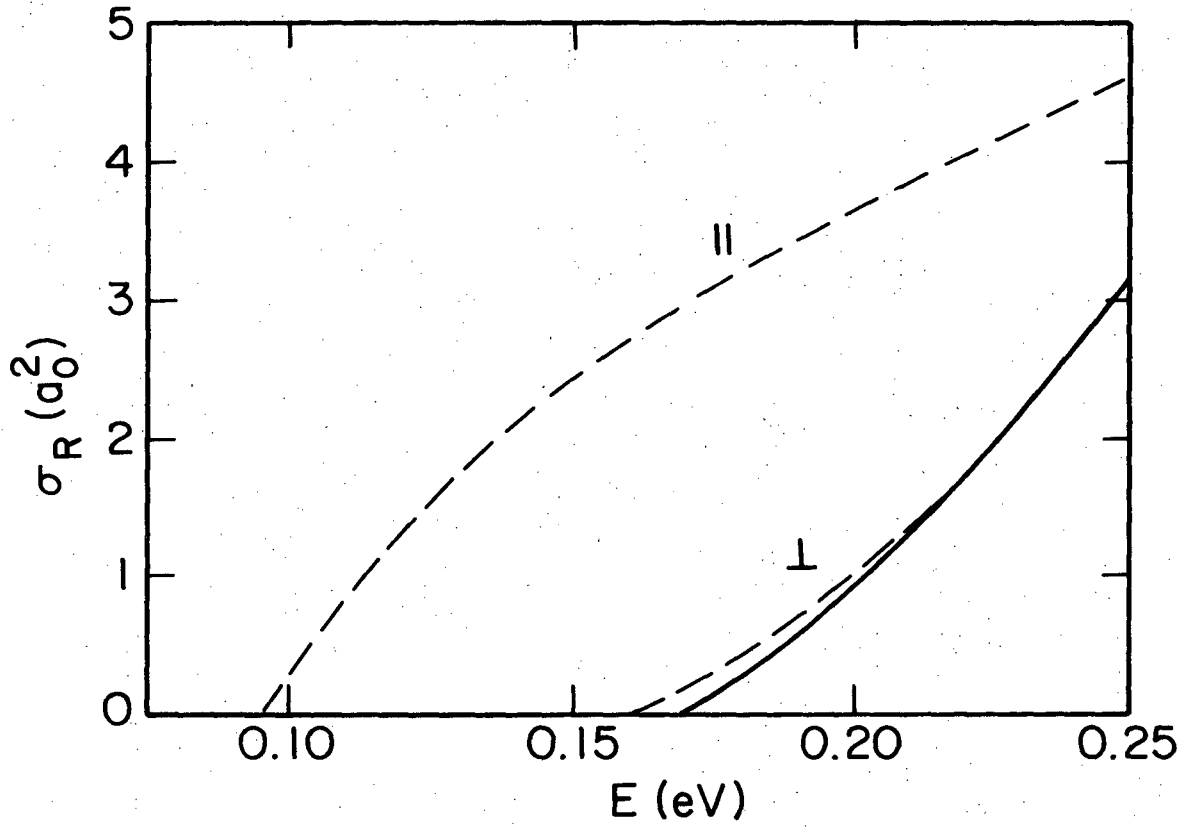
XBL 7810-12114

Figure 7



XBL 7812-14075

Figure 8



XBL 7812-14074

Figure 9

This report was done with support from the Department of Energy. Any conclusions or opinions expressed in this report represent solely those of the author(s) and not necessarily those of The Regents of the University of California, the Lawrence Berkeley Laboratory or the Department of Energy.

TECHNICAL INFORMATION DEPARTMENT  
LAWRENCE BERKELEY LABORATORY  
UNIVERSITY OF CALIFORNIA  
BERKELEY, CALIFORNIA 94720